THE ASTROPHYSICAL JOURNAL, 489:319–330, 1997 November 1

ON TWO THEORIES OF THE CYCLICAL OUTBURSTS OF η CARINAE

RICHARD B. STOTHERS AND CHAO-WEN CHIN
Institute for Space Studies, NASA/Goddard Space Flight Center, 2880 Broadway, New York, NY 10025
Received 1997 February 10; accepted 1997 June 9

ABSTRACT

The star η Carinae is an exceptionally luminous, blue variable that is at least partially evolved and undergoes major outbursts once every 3–6 yr on the average. On the basis of a new grid of stellar evolutionary tracks, we estimate that η Car possessed an initial mass of 150–300 $M_\odot$ and is still burning hydrogen in its core. We test a hypothesis that η Car is repeatedly encountering ionization-induced dynamical instability within its outer envelope. In that case, the star has probably already lost a third of its initial mass, while its surface hydrogen abundance has fallen to about half its original value. Its effective temperature, defined from quasi-static models in the conventional way, is predicted to be 8000 ± 2000 K, but theoretically it might be as high as 200,000 K and so is not accurately known from the models. Although our assumption of hydrostatic equilibrium in the envelope of such an extremely luminous star is crude, the predicted cycles of mass loss agree well with these actually observed. Nevertheless, the models impose requirements before instability first breaks out that seem to be at variance with observations of extremely massive stars: stellar wind mass-loss rates falling too far on the low side and a significant amount of time spent as a B-type supergiant. Our models for η Car itself may be too cool. An alternative destabilizing mechanism, based on an assumed supercritical radiative acceleration of material outward from the photosphere, applies potentially to very luminous, hot stars like η Car, but produces no sustained cycles in our models. However, our models are only quasi-static, not hydrodynamic.

For luminous blue variables generally, we confirm that the mean cycle time is, to a rough approximation, inversely proportional to luminosity. Our results, therefore, justify the use of luminous blue variables as extragalactic distance indicators. Analysis of a simple one-zone model supports our adopted criterion for dynamical instability and hence at least our theoretical results for ordinary luminous blue variables with low and moderate luminosities.

Subject headings: stars: evolution — stars: individual (η Carinae) — stars: interiors — stars: oscillations — stars: variables: other (luminous blue variables)

1. INTRODUCTION

The star η Carinae is a very luminous, dust-enshrouded variable that has attracted much observational and theoretical attention since its great optical outburst in 1843. Its true nature, however, remains a mystery. The central object has been thought to be a massive pre–main-sequence star (Gratton 1963); a massive star in (or just beyond) the main-sequence phase and undergoing (or having undergone) nuclear-energized pulsations in its core (Burbidge 1962; Tammann & Sandage 1968; Burbidge & Stein 1970; Talbot 1971; Davidson 1971; Hoyle, Solomon, & Woolf 1973; Humphreys & Davidson 1979; Davidson, Walborn, & Gull 1982; Doom, De Greve, & de Loore 1986); a massive post–main-sequence supergiant experiencing a violent atmospheric instability (Andriesse, Packet, & de Loore 1981) or an envelope dynamical instability (Stothers & Chin 1983, 1993; Maeder 1983, 1989, 1992) or possibly a multimodal pulsational instability (Glatzel & Kiriakidis 1993b; Kiriakidis, Fricke, & Glatzel 1993); a peculiar slow nova (Aller 1954; Payne-Gaposchkin 1957); a slow supernova (Thackeray 1956; Zwicky 1965; Rodgers & Searle 1967); a pulsar embedded in a supernova remnant (Ostriker & Gunn 1971; Borgwald & Friedlander 1993); and a compact object accreting matter from, or merging with, a companion star (Bath 1979; Warren-Smith et al. 1979; Tutukov & Yungel'son 1980; Viotti et al. 1989; Gallagher 1989; van Genderen, de Groot, & Thé 1994; van Genderen et al. 1995; Damineli 1996).

Objections to many of these hypotheses can be raised. A pre–main-sequence star is easily ruled out because the surrounding nebula, the so-called homunculus (Gaviola 1950), does not consist of undisturbed gas and dust but, rather, is a young, expanding gas and dust cloud (Viotti & Andriesse 1981) that shows overabundances of helium (Allen, Jones, & Hyland 1985; Davidson et al. 1986) and of nitrogen (Davidson et al. 1982, 1986; Burgarella & Paresce 1991; Hamann et al. 1994). The hypothesis that the great outburst in 1843 was due to a nova explosion or a supernova explosion is now also generally discounted, on the grounds of the near-constancy of the star's bolometric luminosity from at least 1860 to the present (van Genderen & Thé 1984). Moreover, no central pulsar has been discovered despite searches for fast optical oscillations (Lasker & Hesser 1972). There is also no measurable polarized, nonthermal radio emission from the object (White et al. 1994).

It is improbable that the cyclical outbursts in η Car have a pulsational origin. Nuclear-energized pulsations can occur in a very massive star only if it lies close to the zero-age main sequence (ZAMS). The half-day period that theory predicts for very massive ZAMS stars (Stothers 1992; Stothers & Chin 1993; Glatzel & Kiriakidis 1993a) is much shorter than any known or suspected periodicity in η Car; the shortest ones mentioned are 52.4 and 58.6 days (van Genderen et al. 1994, 1995; Sterken, de Groot, & van Genderen 1996). As for the strange mode pulsations which have been predicted for massive stars by Glatzel & Kiriakidis (1993b) and by Kiriakidis, Fricke, & Glatzel (1993), their excitation occurs over too broad a region of the Hertzsprung-Russell (H-R) diagram to be specific to η Car. But η Car shares many characteristics with the stars now classified as luminous blue variables (LBVs) (Payne-Gaposchkin 1957; Tammann & Sandage 1968; Thackeray 1974; Humphreys & Davidson 1979, 1994; Conti 1984). The strange modes predicted for LBVs are possibly excited strongly enough to eject matter off the surface (Langer et al. 1994). On the other hand, these modes theoretically exist far outside the region of LBVs, too, and do not correctly predict most of the observational properties of LBVs (Stothers & Chin 1996). It is unlikely that they would account any better for η Car. They may play a role in the observed microvariability, however.

Whether the central core of η Car consists of a close binary system is difficult to determine. It is possible that some of the light variation of η Car arises from an eclipse or a binary interaction event. Proposed orbital periods range from 52.4 days (van Genderen et al. 1994, 1995) to 5.52 yr (Damineli 1996). Although no classical LBV is known to be an interacting binary system (Humphreys & Davidson 1994), the Wolf-Rayet or Op double-star system HD 5980 undergoes LBV-type eruptions and has a luminosity comparable to η Car's; its orbital period is 19.3 days (Koenigsberger et al. 1995; Barbá et al. 1995). In η Car, and perhaps also in HD 5980, we suspect that the LBV-type eruptions may not be immediately related to the proposed duplicity. Rather, a prior close binary mass exchange induced by Roche lobe overflow could have rid the primary star of matter as effectively as a strong stellar wind does. With most of the envelope gone, the stellar remnant evolves into an LBV. Another possible reason for disbelieving a critical role for duplicity is that all of the known extremely luminous nonexplosive stars exhibit typical LBV behavior; these objects include η Car in the Galaxy, HD 5980 in the Small Magellanic Cloud, AF And in M31, V12 in NGC 2403, and, possibly, SN 1961V in NGC 1058. Nevertheless, a binary hypothesis is still entirely viable for η Car.

In the present paper, we explore the possibility that η Car is a main-sequence or post–main-sequence star that has already lost a large amount of mass. For simplicity (but without too much loss of generality) we suppose that the matter came off as the result of a strong stellar wind, not of a binary interaction. The currently unstable condition of η Car is attributed either (1) to a classical ionization-induced dynamical instability in the outer envelope of the star or (2) to an outward-directed pressure force in the star's atmosphere that exceeds the local gravitational force.

The onset of classical ionization-induced dynamical instability can be calculated more or less precisely, and offers no insurmountable theoretical problems. It has already worked well in accounting for ordinary LBVs (Stothers & Chin 1996). Objections to it raised by Glatzel (Langer et al. 1994; Glatzel, Kiriakidis, & Fricke 1994) have been based on stellar models with either too much or too little mass loss to become dynamically unstable, and, more seriously, on the erroneous use of the *nonadiabatic* pulsation period to test for dynamical instability (see § 4.1 and Appendix).

Atmospheric instabilities are still in the highly speculative stage, at least as to their possible consequences. A number of authors have proposed that a very strong outward-directed radiation pressure force in the atmosphere might exceed gravity at some point and lead to enhanced mass loss (Davidson 1971; Appenzeller 1986, 1989; Lamers 1986; Lamers & Fitzpatrick 1988). This should occur for the first time near the ZAMS for stars of very high luminosity. The simultaneous effect of a steep gradient of turbulent pressure in the atmosphere (de Jager 1980), however, is expected to be superseded in importance by the purely radiative acceleration mechanism (de Jager 1984; Blomme, Vanbeveren, & Van Rensbergen 1991) and so will be ignored here. Three other potential atmospheric mechanisms will also be neglected, because they apply only at very cool effective temperatures (<8000 K), at which they are superseded by ordinary ionization-induced dynamical instability in the present applications. These mechanisms are the following: a large density inversion deep in the convective atmosphere (Bisnovatyi-Kogan & Nadyoshin 1972; Bisnovatyi-Kogan 1973; Maeder 1989, 1992), a strong acoustic flux generated by turbulent convection (Fusi-Pecci & Renzini 1975), and a strong, stochastic velocity field that characterizes the turbulent mass elements rising from the photosphere (Andriesse 1979; Andriesse et al. 1981).

Arrangement of the present paper is as follows. In § 2 the needed observational data for η Car are reviewed and synthesized. Physical input data to the stellar models are briefly described in § 3, while § 4 discusses in detail the two most important destabilizing mechanisms considered here. Evolutionary tracks based on these two destabilizing mechanisms are presented in §§ 5 and 6, including a critical comparison with the relevant observations of η Car. Potential extragalactic applications of our results for η Car and for other LBVs are suggested in § 7. Finally, § 8 summarizes and discusses our main conclusions.

2. OBSERVATIONAL PARAMETERS OF η CAR

2.1. *Luminosity*

Eta Carinae lies along the line of sight to an open cluster of early O stars, Trumpler 16 (Tr 16), which excites the central part of a giant H II region known as the Carina Nebula (NGC 3372). The physical association of η Car with NGC 3372, and hence with Tr 16, is now very well established (Walborn & Hesser 1975; Walborn & Liller 1977; Allen 1979). Published distances to Tr 16, based on modern multicolor photometry and MK spectral types of its O stars, are listed in Table 1. Some of the scatter of the 20 published distances comes from making different assumptions about the reddening law for Tr 16, which may be anomalous, but the mean distance and the modal distance are both 2.5 kpc.

An independent way of deriving the distance is to calculate the so-called nova parallax, based on the rate of outward motion of the observed ejecta from the central object, together with the known time of expulsion. For η Car, this calculation has been done by combining the expulsion time with the measured radial velocity of a selected dust condensation, in conjunction with either that condensation's measured proper motion (Thackeray 1961; Gratton 1963; Gehrz & Ney 1972; Gehrz et al. 1973; Walborn, Blanco, & Thackeray 1978; Meaburn, Walsh, & Wolstencroft 1993) or its total angular separation from the central object (Thackeray 1953; Allen & Hillier 1993). The five resulting distance determinations published since 1972 give excellent agreement, 2.1–2.5 kpc, and average 2.3 kpc.

In what follows, we adopt $r = 2.4 \pm 0.1$ kpc for η Car.

TABLE 1

PUBLISHED DISTANCES TO TR 16 IN THE CARINA NEBULA

r (kpc)	Reference
2.5......	Hoffleit 1956
1.7......	Becker 1960
2.5......	Faulkner 1963
2.8......	Feinstein 1963
1.5......	Gratton 1963
2.5......	Feinstein 1969
2.5......	Thé & Vleeming 1971
2.6......	Feinstein et al. 1973
2.6......	Walborn 1973
2.4......	Herbst 1976
2.4......	Forte 1978
2.7......	Humphreys 1978
2.8......	Thé et al. 1980
2.7......	Turner & Moffatt 1980
2.4......	Forte & Orsatti 1981
2.5......	Levato & Malaroda 1982
2.5......	Tapia et al. 1988
3.2......	Kaltcheva & Georgiev 1993
3.2......	Massey & Johnson 1993
2.6......	Shobbrook & Lyngå 1994

The total dereddened apparent flux received from the object (van Genderen & Thé 1984) translates into a bolometric luminosity of $\log (L/L_{\odot}) = 6.69 \pm 0.06$, or $M_{\rm bol} = -12.0 \pm 0.2$. It is now known that the central core of η Car is not multiple, but consists of a single star or, just possibly, a binary star (Davidson et al. 1995). Therefore, the minimum luminosity, if η Car is a binary with two equal components, would be $\log (L/L_{\odot}) = 6.39 \pm 0.06$, or $M_{\rm bol} = -11.2 \pm 0.2$, for one of the components. The assigned errors take into account the uncertainties of the distance, interstellar extinction, and spectral flux curve; most of the observed flux emerges in the infrared as a result of the redistribution of the central starlight by the surrounding dust.

2.2. *Effective Temperature*

For a long time, the line spectrum displayed by the inner part of η Car was attributed to the photoionization of gas lying at or near the stellar photosphere (possibly within the opaque wind). An effective temperature of $(2\text{–}4) \times 10^4$ K had been inferred (Pagel 1969; Davidson 1971; Pottasch, Wesselius, & van Duinen 1976; Allen, Jones, & Hyland 1985; Davidson et al. 1986; Men'schikov, Tutukov, & Shustov 1989; Hillier & Allen 1992; Tovmasyan, Oganesyan, & Epremyan 1993); however, a value as low as 7500 K was also suggested (Andriesse et al. 1981). More recently, the view that the gas is collisionally ionized has come to prevail (Viotti et al. 1989; Borgwald & Friedlander 1993; Corcoran et al. 1995; Cox et al. 1995; Davidson et al. 1995; Levenson et al. 1995). Based on millimeter-wave, X-ray, and [Cr]-line observations, this improved view implies that an effective temperature cannot at present be assigned to the underlying star. However, spectral continuum observations, in conjunction with the second law of thermodynamics, suggest that the effective temperature must be at least 15,000 K (Davidson et al. 1995).

2.3. *Chemical Anomalies*

Helium is believed to be overabundant in the homunculus (Allen et al. 1985) and in the outer "S condensation" (Davidson et al. 1986). Similarly, nitrogen appears overabundant as well (Davidson et al. 1982, 1986; Burgarella & Paresce 1991; Hamann et al. 1994). Since, however, the visible gases are mostly shock-heated, the degree of overabundance is very difficult to estimate. This renders questionable the specific nebular abundance of helium, $Y \approx 0.4$, that Davidson et al. (1986) have determined.

2.4. *Mass Loss*

The present rate of mass loss from the central object in η Car falls somewhere in the range $(1\text{–}3) \times 10^{-3}\ M_{\odot}\ {\rm yr}^{-1}$, according to several recent independent determinations (Davidson et al. 1986, 1995; White et al. 1994; Cox et al. 1995). In the great outburst of 1843, the rate of mass loss was either about the same as today's rate or, more probably, somewhat higher. The 1843 rate has been estimated variously as $4 \times 10^{-3}\ M_{\odot}\ {\rm yr}^{-1}$ (van Genderen & Thé 1984), $2 \times 10^{-2}\ M_{\odot}\ {\rm yr}^{-1}$ (Hyland et al. 1979), $7.5 \times 10^{-2}\ M_{\odot}\ {\rm yr}^{-1}$ (Andriesse, Donn, & Viotti 1978), and $\sim 10^{-1}\ M_{\odot}\ {\rm yr}^{-1}$ (Davidson 1989).

Proper-motion studies show that the homunculus was produced by the short series of eruptions around 1843, with lesser contributions being added afterward (Currie et al. 1996). Its mass is uncertainly estimated as 0.15 $M_{\odot}$ (van Genderen & Thé 1984) or as falling in the range 2–10 $M_{\odot}$ (Andriesse et al. 1978; Hyland et al. 1979; Davidson 1989). Difficulty in estimating the mass arises from the nonspherical form of the object—two symmetric, hollow, osculating lobes with a thin disk lying between them (e.g., Humphreys & Davidson 1994). This may indicate rotation, duplicity, or a magnetic field in the underlying star. There is also the need to assign a specific value of the gas-to-dust ratio (usually taken to be ~ 100), the dust mass alone having been measured. The dense clumpy material immediately surrounding the central object probably contains only $\sim 10^{-2}\ M_{\odot}$ (Smith et al. 1995).

2.5. *Variability*

The visual photometric history of η Car consists of a few scattered observations before 1822 (Gratton 1963) and more nearly complete coverage since then. In 1822, η Car shone at magnitude 2. It reached its greatest recorded visual brightness, -1 mag, in 1843 during an extraordinary outburst. By 1870, it had faded to magnitude 8, where it remained, with some variability, until about 1940. Since that time, η Car has gradually brightened to its present magnitude 6.

In color, η Car was reddest around 1843. Subsequently, it has slowly (and probably irregularly) grown bluer, owing to a gradual dispersal of the ejected dust cloud (van Genderen & Thé 1984).

Smaller scales of variability can also be detected. Table 2 lists the dates of all the known light maxima, according to various published sources. Some of these maxima may be false detections. On the other hand, the list may be incomplete owing to inadequate observations during some periods. A good way of checking the suggested maxima is by spectroscopic means, to determine whether the maxima exhibit the characteristic spectral behavior of LBV (S Doradus–type) shell-ejection events. Spectroscopic observations are available for only five light maxima since 1889 (Table 2), but confirm the existence of small mass ejections. In addition, shell events occurred in 1948 and 1965 (Damineli 1996), at times for which adequate photometric observations are unavailable.

TABLE 2

OBSERVED MAXIMA OF η CAR

Year	Observed Feature	Reference
1827......	Light peak	1
1838......	Light peak	2
1843......	Highest light peak	2
1856......	Light peak	2
1862......	Light peak?	2, 3, 4
1871......	Light peak?	2
1889......	Light peak; shell event	2, 5, 6, 7
1942......	Light peak	6
1948......	Shell event	8
1952......	Light peak; shell event	7, 9, 10
1955......	Light peak?	10
1958......	Light peak?	10
1961......	Light peak?	10
1965......	Shell event	8
1976......	Light peak	11, 12
1981......	Light peak; shell event	8, 11, 12
1987......	Light peak; shell event	8, 11, 12
1992......	Light peak; shell event	8, 12

REFERENCES.—(1) Gratton 1963; (2) Innes 1903; (3) Polcaro & Viotti 1993; (4) Feast, Whitelock, & Warner 1994; (5) Hoffleit 1933; (6) O'Connell 1956; (7) Payne-Gaposchkin 1957; (8) Damineli 1996; (9) de Vaucouleurs & Eggen 1952; (10) Feinstein & Marraco 1974; (11) van Genderen, de Groot, & Thé 1994; (12) Whitelock et al. 1994

Depending on the size of the outburst, different mean intervals between outbursts can be derived. On the largest scale, the big outbursts are possibly several centuries apart, because, in addition to the great outburst in 1843, another big eruption may have occurred during the fifteenth century, according to proper-motion studies of distant dust condensations around η Car (Walborn et al. 1978). For more moderate-sized outbursts, Payne-Gaposchkin (1957) has suggested a mean interval of 15–16 yr, at least during the period 1820–1900. On the smallest scale, the published suggestions differ: 1–3 yr cycles, claimed to have occurred during 1974–1992 (van Genderen et al. 1994), ~ 3 yr cycles during 1952–1973 (Feinstein & Marraco 1974), 5 yr cycles during 1975–1994 (Whitelock et al. 1994), and 5.52 yr cycles during 1948–1995 (Damineli 1996).

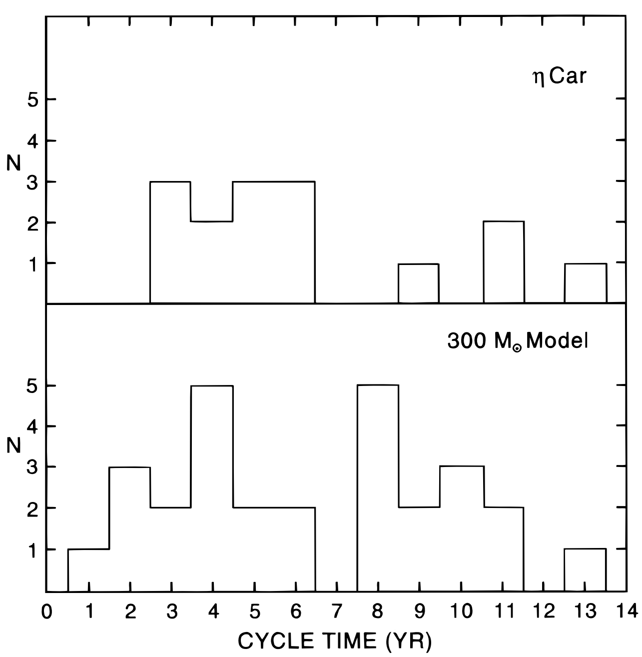

FIG. 1.—Histogram of measured cycle times for (*a*) η Car and (*b*) stellar models of initially 300 $M_\odot$ with $w = 0.1$ in the first phase of dynamical instability.

Given the spectroscopic evidence, however, there seems no good physical reason for treating the outbursts differently according to how large their visual ranges were. Therefore, we propose accepting the list of 18 outbursts in Table 2 as being more or less complete, or at least as being representative, for the period 1822–1995. A histogram of the time intervals between outbursts is shown in the upper panel of Figure 1 for intervals shorter than 14 yr (only two are longer than this). Two-thirds of these representative cycle times fall in the range 3–6 yr. The scatter among them is probably real and can account for the differing periodicities claimed by different authors.

3. INPUT PHYSICS FOR THE STELLAR MODELS

Physical assumptions made for our present stellar models are the same as those adopted in our recent series of papers. Specifically, the initial hydrogen and metal abundances by mass are taken to be $X = 0.70$ and $Z = 0.03$. Opacities, κ, come from Iglesias, Rogers, & Wilson (1992). For initial stellar masses, we choose here 150, 210, and 300 $M_\odot$. Since the rate of radiatively driven stellar wind mass loss from objects so massive is unknown, we simply adopt the analytic formula fitted to the observational rates of mass loss for less massive stars given by Nieuwenhuijzen & de Jager (1990), but arbitrarily modified here by a constant scale factor w. To keep the physics uncomplicated, we have ignored convective-core overshooting, semiconvection, rotation, and magnetic fields.

Very recently, de Koter, Heap, & Hubeny (1997) have estimated very large mass-loss rates for the most massive stars in the essentially unevolved cluster R136a in the Large Magellanic Cloud. These stars possess masses of $\sim 100\ M_\odot$, and their rates of mass loss correspond to $w \approx 3$, at least in their present state near the ZAMS. If these estimates hold up generally and a comparable value of w applies at higher stellar masses, the consequences for our tentative identification of the instability mechanism in η Car would be profound and evidently negative (§ 5).

4. DESTABILIZING MECHANISMS

4.1. *Ionization-induced Dynamical Instability*

Very massive stars generate such high luminosities that radiation pressure inside them is large compared to gas pressure. Consequently, the first generalized adiabatic exponent, Γ_1, is close to the value 4/3 throughout most of the interior of these stars. In the subphotospheric layers of partial ionization of hydrogen and helium, Γ_1 drops well below 4/3. It follows that only a small ionization zone is needed to reduce the pressure-weighted volumetric average, $\langle\Gamma_1\rangle$, below 4/3 in the outer envelope of a very luminous star. When this happens, the outer envelope is ripe for dynamical instability (Ledoux 1958).

A crucial additional requirement is that the region with $\langle\Gamma_1\rangle$ less than 4/3 be only loosely coupled to the rest of the star, so that large-amplitude perturbations are effectively confined to the quasi-isolated outer region and are not quenched by the stable layers beneath. Because the atmosphere is not an isolated part of the total stellar structure, it cannot be destabilized by this mechanism even it it has

$\langle \Gamma_1 \rangle$ less than 4/3 (see Tuchman, Sack, & Barkat 1978; Lobel et al. 1992). However, underneath the layers of partial ionization of hydrogen and helium lies a thin zone with a very large opacity due primarily to multiple iron lines. Such a high opacity greatly increases the local radiation pressure, reduces the local gas density, and creates a kind of "quasi-photosphere" at a temperature of $\sim 2 \times 10^5$ K. When $\langle \Gamma_1 \rangle$ in the overlying layers of the star falls below 4/3, dynamical instability breaks out and these layers become unbound from the rest of the star.

Our adopted criterion for dynamical instability is derived from an approximate solution of the linearized wave equation for adiabatic radial pulsations. However, the exact solution of this equation gives nearly the same onset point for dynamical instability (Stothers & Chin 1993). At this stage, the inverse of the adiabatic pulsation period vanishes. A concern might be that adiabatic pulsation theory is being used in a highly nonadiabatic region of the star. For at least the nonadiabatic one-zone model of a stellar envelope, however, the rigorously correct threshold of dynamical instability is in fact given by the adiabatic condition $\Gamma_1 = 4/3$ (Baker 1966), and this is very likely to be general (Tuchman et al. 1978). Although the adiabatic pulsation period is purely imaginary in the dynamically unstable regime (implying aperiodic expansion), fully nonadiabatic hydrodynamical calculations reveal that dynamical instability actually proceeds through the development of violent relaxation oscillations of rapidly growing amplitude that eventually expel mass from the star's surface. The period of the relaxation oscillations in our models (Stothers & Chin 1993) can be represented approximately by the fitted formula

$$\Pi(\mathrm{yr}) \approx 2 \times 10^{-4} (M/M_\odot)^{-1/2} (R/R_\odot)^{3/2} .$$

This excited strange mode is a nonadiabatic phenomenon, superimposed on the quasi-adiabatic expansion of the outer envelope (see Appendix). Typically, Π is found to be ~ 0.5 yr, which is larger by a factor of 10 than the free-fall collapse time, but smaller by a factor of 10 than the thermal timescale.

Whenever a stellar model along an evolutionary track is determined to be dynamically unstable, we estimate the associated rate of mass loss in the following way. An arbitrary rate, somewhat larger than the quiescent stellar wind mass-loss rate, is assigned in the next model. If the star continues to be unstable, the rate is then increased until stability is achieved within a few models. In general, we find that only a limited range of enhanced mass-loss rates leads to a satisfactory solution in which the star evolves back and forth between dynamically stable and unstable states. Although the successive cycle times are not identical, a mean period can be determined by using a simple average of the cycle times. This mean period is found to depend little on the particular rate of mass loss that is selected within the allowed range. On the other hand, if the rate is too large, the star simply becomes stable for an extended length of time. This evolutionary behavior of the star's envelope follows the pattern already established for stellar models of smaller initial mass (Stothers & Chin 1983, 1995).

Many of the relevant physical timescales in these very luminous stellar models not only are very short but also are roughly of the same order of magnitude. Each timescale contributes to determining the characteristic length of the recurring cycles of envelope instability, whose successive stages consist of eruption, hydrostatic adjustment, thermal adjustment, and reexpansion. In fact, the sharp physical distinctions that normally exist between the phenomena of mass loss, dynamical instability, and secular instability become blurred when all three phenomena are interacting and have comparable timescales. We should also point out the comparably short overturning times of turbulent convection in the convectively unstable hydrogen, helium, and iron ionization zones.

Under these circumstances, the outer envelope of η Car may never be in much more than approximate hydrostatic equilibrium. This complication introduces some uncertainty into our assumption of static surface boundary conditions. Possibly, no true photosphere exists. Even the noneruptive mass-loss rate observed for η Car is more than sufficient to form an opaque stellar wind and hence a permanent pseudophotosphere. Underneath the wind, disturbed conditions must extend into the interior, since an amount of envelope mass equal to $\delta M = |dM/dt| \tau_{\mathrm{dyn}}$ must supply the wind on a timescale, τ_{dyn}, of only months. This implies that a hot layer lying δM below the pseudophotosphere might approximate the true photosphere, which could therefore be almost as hot as the "quasiphotosphere" at $T \approx 2 \times 10^5$ K. Furthermore, the heavy mass loss from the stellar surface produces a back-reaction on the interior that, mathematically speaking, is the result of total energy conservation and total momentum conservation. The physical consequences are a small luminosity drop and a recoil pressure (Forbes 1968). Although these factors turn out to be negligible for the surface parameters of η Car, a back-warming of an unknown amount will also occur. Finally, the predicted relaxation oscillations of the envelope should not affect the luminosity very much (Stothers & Chin 1993), but should puff up the outer layers and cause the effective temperature of the photosphere (at some characteristic radius R) to change as $R^{-1/2}$. In sum, all of these uncertainties do not much affect our calculations of the luminosity and evolution of the underlying star, but do call into question the star's assigned "effective temperature."

One may ask, therefore, whether our adopted criterion for dynamical instability has much validity when it is applied to a star that may be out of hydrostatic and thermal equilibrium. Our answer is that, because η Car shows continuous cycles, the star must be returning to more or less the same configuration during its approximate quiescent state (§ 5). Whatever the appropriate modified criterion for dynamical instability may be in these circumstances, the threshold for stability will still be crossed episodically, and this will create mass-loss cycles. A somewhat changed criterion will lead only to a somewhat different effective temperature at the stability threshold. Since the effective temperature is uncertain for other reasons, our theoretical results can be expected to be flawed mainly in regard to the interoutburst threshold effective temperature, but not so much otherwise.

4.2. *Supercritical Radiative Acceleration of Matter*

Although the quiescent stellar wind in a hot luminous star is mainly radiation-driven by absorption in the star's numerous spectral lines (Castor, Abbott, & Klein 1975; Lucy & Abbott 1993), a further enhancement will occur if the local Eddington luminosity limit ($L_E = 4\pi cGM/\kappa$) is exceeded in the photosphere. If this limit happens to be exceeded only in the overlying optically thin layers, the enhanced mass loss will be slight, whereas below the photosphere the radiative diffusion approximation applies, so that spectral line effects act like continuum effects and line-driven mass loss will not occur (Lamers & Fitzpatrick 1988). In our calculations, all subphotospheric layers in which the Eddington limit is locally violated (even inside our most luminous stellar models) do no drive off matter but become turbulently convective without the mean convective velocities anywhere exceeding sound speed (Stothers & Chin 1993). Therefore, it is necessary to look to the formation of a pseudophotosphere in order to enhance the rate of mass loss.

The presently observed mass-loss rate of η Car, $\sim 10^{-3}$ $M_{\odot}$ yr^{-1}, is large enough (by 2 orders of magnitude) to form a pseudophotosphere inside the optically thick, quiescent stellar wind (Davidson 1987; Lamers 1987; Leitherer et al. 1989; de Koter, Lamers, & Schmutz 1996). Consequently, the difficulties encountered by the radiative acceleration mechanism in explaining the visual light variations of the less luminous LBVs, viz., observed stellar luminosities that are too low (Lamers & Fitzpatrick 1988) and observed mass-loss rates that appear too small to form a substantial pseudophotosphere (de Koter et al. 1996), do not apply to η Car.

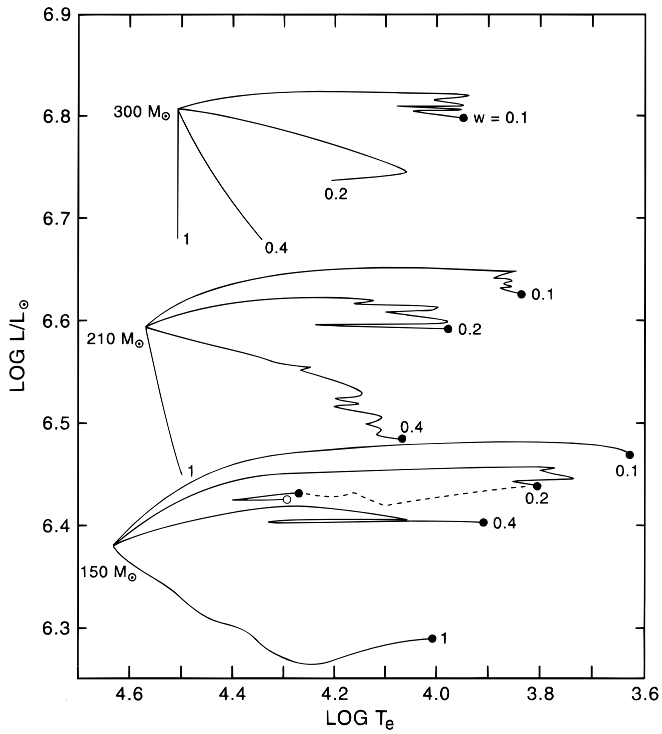

FIG. 2.—Theoretical H-R diagram showing evolutionary tracks running from the ZAMS to the start of the first phase of dynamical instability or, in some cases, to a stage well before the start. The initial stellar mass and the stellar wind mass-loss parameter w are indicated. A dot marks the start of dynamical instability. In the case of 150 $M_{\odot}$ with $w = 0.2$, the subsequent evolution is shown, with a second dot indicating the end of the first phase of dynamical instability and with an open circle denoting the start of the second phase of dynamical instability.

5. STELLAR MODELS WITH IONIZATION-INDUCED DYNAMICAL INSTABILITY

Evolutionary tracks running up to the first stage of ionization-induced dynamical instability are plotted on the H-R diagram in Figure 2. Because rates of stellar wind mass loss characterized by $w \geq 1$ are extremely large for initial stellar masses above 150 $M_{\odot}$, stripping of the outer radiative envelope proceeds nearly in tandem with the thermonuclear depletion of hydrogen in the inner convective core. The consequence is a quasi-homogeneous evolution of the mass-losing star (Simon & Stothers 1970; Stothers & Chin 1979 Maeder 1980). Such objects fail to become dynamically unstable. Therefore, we have also assigned smaller rates for the stellar wind mass loss, $w = 0.1$, 0.2, and 0.4, and have applied these rates to all three initial stellar masses.

Above ~ 120 $M_{\odot}$, ionization-induced dynamical instability first occurs during the main-sequence phase and always at some effective temperature lower than 12,000 K. Although this limiting effective temperature also applies for smaller initial masses (Stothers & Chin 1994), the main sequence at smaller masses is not so wide, and, in consequence, dynamical instability there begins only after the main-sequence phase is completed. Table 3 compares the surface properties of our new models in the ZAMS stage with the surface properties of the models at the first stage of dynamical instability. A peculiar feature to be noted is that the rate of quiescent stellar wind mass loss at the onset of instability always lies near 1.5×10^{-4} $M_{\odot}$ yr^{-1}, whereas the rate in the ZAMS stage ranges from 3×10^{-6} to 3×10^{-5} $M_{\odot}$ yr^{-1}. We do not regard this convergence of the rates as anything more than a chance coincidence.

For one of our evolutionary tracks, the case of 150 $M_{\odot}$ with $w = 0.2$, we carried out additional calculations past the phase of core hydrogen burning into the phase of core

TABLE 3

EVOLUTIONARY MODELS OF STARS

		ZAMS STAGE			ONSET OF DYNAMICAL INSTABILITY					
INITIAL $M/M_{\odot}$	w	$\log (L/L_{\odot})$	$\log T_e$	$-\dot{M}$ ($M_{\odot}$ yr^{-1})	$M/M_{\odot}$	X_c	$X_{\rm surf}$	$\log (L/L_{\odot})$	$\log T_e$	$-\dot{M}$ ($M_{\odot}$ yr^{-1})
150......	0.1	6.38	4.63	2.6(−6)	114	0.07	0.56	6.47	3.63	1.5(−4)
	0.2	6.38	4.63	5.2(−6)	100	0.11	0.42	6.44	3.81	1.4(−4)
	0.4	6.38	4.63	1.1(−5)	81	0.01	0.26	6.40	3.91	1.6(−4)
	1.0	6.38	4.63	2.6(−5)	56	0	0.12	6.29	4.01	1.7(−4)
210......	0.1	6.59	4.57	7.8(−6)	144	0.14	0.40	6.63	3.84	1.3(−4)
	0.2	6.59	4.57	1.6(−5)	111	0.07	0.20	6.59	3.98	1.4(−4)
	0.4	6.59	4.57	3.1(−5)	84	0.03	0.10	6.48	4.07	1.2(−4)
300......	0.1	6.81	4.51	2.3(−5)	196	0.23	0.34	6.80	3.94	1.8(−4)

NOTE.—X_c and $X_{\rm surf}$ refer to the central and surface abundances of hydrogen by mass.

helium burning. The dashed line in Figure 2 indicates the dynamically unstable stages up to and beyond the end of core hydrogen burning. Afterward, the star becomes very blue and stabilizes. A quarter of the way through central helium depletion, after having begun to reexpand, the star encounters dynamical instability again at very nearly the same effective temperature, 20,000 K, where the instability previously ended. The star's mass is now 64 $M_\odot$ and its surface hydrogen abundance, $X_{\rm surf}$, is 0.02. These post–main-sequence developments, including the noticeably relaxed threshold of effective temperature for dynamical instability, are due to a significantly decreased envelope mass.

Eta Carinae is unlikely to be in the second phase of dynamical instability. In the case of initial stellar masses above $\sim 120\ M_\odot$, this phase is shorter by an order of magnitude than the first phase. Furthermore, during the second phase, the stellar models are practically hydrogen-free, whereas observed fresh ejecta from η Car show strong hydrogen lines (Payne-Gaposchkin 1957). Finally, if hydrogen were of very low abundance in η Car, the pseudo-photosphere formed during an eruption ought to attain a minimum effective temperature of $\sim 13,000$ K, which is the recombination temperature of singly ionized helium. But observationally, the reddish color of η Car in 1843 and its F-type spectrum in 1893 are more consistent with the recombination temperature of hydrogen, ~ 8000 K (Davidson 1987). Metal opacities, however, are also important and may allow a lower temperature to be reached.

For these reasons, we will turn our attention now to only the first phase of dynamical instability. As representative of this phase, we discuss an early stage, although tests show that later stages behave in a similar manner. In the case of our models for 150 $M_\odot$ with $w = 0.2$, three or four consecutive cycles are found to be inevitably followed by a long interval of stability before the cycles break out anew. This broken pattern fails to resemble the observed cyclical behavior of η Car. Also, the mean period of the theoretical cycles is somewhat too long, 5–7 yr.

The cycles recur at a more rapid pace over a much more extended length of time for our models of 300 $M_\odot$ with $w = 0.1$. A histogram of the derived cycle times is displayed in Figure 1, where our results compare very well with the observed distribution of cycle times for η Car. A typical theoretical cycle is ~ 4 yr long. As was the case at lower stellar masses (Stothers & Chin 1995), the amplitudes in the H-R diagram are quite small, the average effective temperature amplititude being 0.003 dex and the average luminosity amplitude being less than 3×10^{-5} dex. These results refer, of course, to a quasi-static calculation of the star's cycles. During the dynamically unstable, eruptive stages, the violent relaxation oscillations of the envelope should inflate the outer layers and induce periodic excursions of the radius and effective temperature. It is likely that these fluctuations would be masked beneath the pseudo-photosphere of the opaque expanding cloud.

Because the various physical timescales in the outer envelope are so similar, it is sometimes difficult to distinguish cause and effect. In Figure 3, we plot the secular evolution of the effective temperature of the star over two successive cycles. Although the absolute scale of effective temperatures is not reliable (§ 4.1), the computed relative changes from cycle to cycle are probably realistic. Open circles denote dynamically stable models, and filled circles represent dynamically unstable models with enhanced mass loss. To reduce confusion in interpreting the results, the rate of quiescent stellar wind mass loss has been set to zero in this particular stretch of the evolutionary track. For the dynamically unstable models, the rate of eruptive mass loss has been set to $2 \times 10^{-4}\ M_\odot\ {\rm yr}^{-1}$ in one computational run and to $2 \times 10^{-2}\ M_\odot\ {\rm yr}^{-1}$ in a second. Rates that lie outside this range do not lead to any cycles. Despite the large difference between the two adopted rates, the results for the derived cycles are very similar to each other and hence the properties of the cycles should be regarded as reliably established.

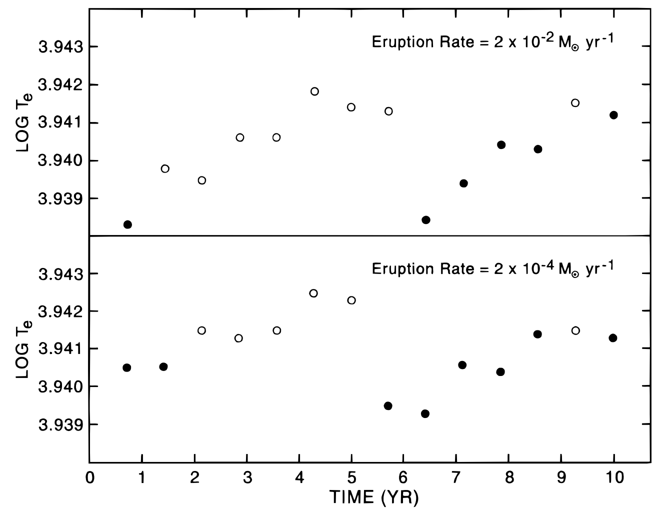

FIG. 3.—Effective temperature vs. time for two cycles of mass loss during the first phase of dynamical instability. Initial stellar parameters are $M = 300\ M_\odot$ and $w = 0.1$. During this segment of the computational runs, the rate of quiescent stellar wind mass loss has been arbitrarily set to zero. Results for two assigned rates of eruptive mass loss are shown. Filled circles denote dynamically unstable models; open circles indicate dynamically stable models. For each panel, the starting time is arbitrary.

Notice that at the end of each cycle the effective temperature does not quite return to its starting value. This slight drift arises from the overall evolution of the star. Although the luminosity changes very slightly over a cycle, the stellar mass drops comparatively quickly, and the consequent increase of the luminosity-to-mass ratio facilitates the onset of dynamical instability. As a result, the critical effective temperature for instability increases with time. If the eruptive mass-loss rate is assumed to be $2 \times 10^{-4}\ M_\odot\ {\rm yr}^{-1}$, the critical effective temperature rises by 0.0005 dex in 7 yr, whereas for the higher rate of $2 \times 10^{-2}\ M_\odot\ {\rm yr}^{-1}$ it increases by 0.002 dex in the same amount of time. Hence the net evolutionary effect of the mass loss is to slowly shift the star blueward on the H-R diagram.

Another interesting feature revealed by Figure 3 is the occasionally superfluous effect of dynamical instability on the actual commencement of the cycles. Sometimes the oscillations of effective temperature persist for one or two cycles even when the eruptive mass loss continues unabated, or sometimes even when there is no ongoing mass loss at all. We have already noted, in our discussion of ordinary LBVs (Stothers & Chin 1996), how remarkably little enhancement of the quiescent mass-loss rate is needed to sustain these cycles. Although oscillatory secular instability is not unknown in stellar evolution calculations (Hansen 1978), it is relatively rare.

The total amount of mass lost per cycle in our models is obviously highly variable. Assuming, on average, $\Delta M = 0.5\,|dM/dt|\,\Delta t$, where dM/dt is the assigned rate of eruptive mass loss and Δt is the mean cycle time, we find $\Delta M \sim 10^{-3}$ to $10^{-1}\,M_\odot$ from our evolutionary models, the chief uncertainty being the rate of eruptive mass loss. These results are generally compatible with what is known about η Car. In addition to the observed average properties of η Car, the variable lengths and variable intensities of the star's major outbursts become more comprehensible in our quasi-stochastic picture of the outbursts.

One puzzle concerning the great 1843 outburst, however, cannot be satisfactorily solved. Around that time, the integrated bolometric magnitude of η Car appears to have been $\sim$2.5 mag brighter than it is today (van Genderen & Thé 1984), whereas according to our theoretical stellar models for LBV eruptions the luminosity ought to be essentially constant at all times. Davidson (1989) has suggested that the excess radiated energy represents the release of internal and kinetic energy stored in the expelled cloud, which shortly before had been part of the underlying star. His estimates, while rough, are compatible with our models but require a large value of the homunculus mass (§ 2.4).

Alternatively, if η Car is an interacting binary system, the excess radiated energy might be attributed to a Roche-lobe overflow event or to an accretion event (§ 1). This would not necessarily conflict with the best current interpretation of the other known outbursts in η Car as having been LBV (S Doradus–type) events.

Despite the success of our models in accounting for the observed cycles, there may exist problems with the prior evolution of the star vis-à-vis observations of very massive stars. These problems will be discussed in § 8.

6. STELLAR MODELS WITH SUPERCRITICAL RADIATIVE ACCELERATION

Two evolutionary tracks were computed under the assumption that enhanced mass loss occurs as a result of supercritical radiative acceleration of matter in the photosphere. Lacking detailed atmospheric models, we have simply guessed from Lamers & Fitzpatrick's (1988) less luminous atmospheric models that supercriticality would exist for $T_e \leq 30{,}000$ K at the luminosities that apply to η Car. Possibly, the true effective temperature limit is somewhat higher, even exceeding the ZAMS effective temperature. But increasing this limit would not alter our results fundamentally.

In our evolutionary track for 300 $M_\odot$ with $w = 0.1$, various enhancements of the mass-loss rate were tried. No cycles ever appeared. Even with a mass-loss rate as high as $10^{-1}\,M_\odot\,\mathrm{yr}^{-1}$, the star evolved steadily cooler, driven by central hydrogen burning in a stage very close to the ZAMS, around a luminosity of $\log\,(L/L_\odot) = 6.8$. Other choices of w made no difference, as the star lies so close to the ZAMS. This mechanism, at least as we have applied it, cannot readily explain η Car.

Another evolutionary track was computed for a lower luminosity, $\log\,(L/L_\odot) = 6.1$, which is near the level where this mechanism could no longer actually operate (Lamers & Fitzpatrick 1988). The corresponding initial stellar mass is 90 $M_\odot$. Although this mass cannot represent η Car, it may refer to AG Car, a less extreme LBV. With similar model assumptions, the evolutionary track for 90 $M_\odot$ does show recurring cycles, having a mean cycle time of 11 yr within a total range of 4–22 yr. The eruptive mass-loss rate, however, has to be made very large in order to overcome the strong secular stability of the star at this very early stage of central hydrogen burning. The theoretically permitted mass-loss rates, all exceeding $10^{-2}\,M_\odot\,\mathrm{yr}^{-1}$, are larger by at least 2 orders of magnitude than the observed eruptive mass-loss rates of AG Car (Wolf & Stahl 1982; Robberto et al. 1993; Leitherer et al. 1994; Lamers et al. 1996). We conclude that the supercritical radiative acceleration mechanism does not, in any obvious way, produce the observed cyclical eruptions of LBVs. On the other hand, our quasi-static models are very limited in their degree of sophistication.

7. EXTRAGALACTIC APPLICATIONS

Mean cycle times for our LBV models of 150 and 300 $M_\odot$ can be compared with those we derived previously for 45 and 90 $M_\odot$. The more massive, and hence more luminous, models show shorter periods, as we had already suspected on the basis of just the two smallest masses. Open circles in Figure 4 exhibit the corresponding period-luminosity relation. Our results are not very sensitive to the choices of effective temperature or even of evolutionary phase along a given track. For example, our numerical experiments at 90 $M_\odot$ yielded $P = 11$ yr near the ZAMS (§ 6) and $P = 10$ yr near the end of central helium burning (Stothers & Chin 1995).

Observations of LBVs suggest a very similar relation between the mean period and the luminosity (Stothers & Chin 1995). The observational relation is also displayed in Figure 4. Unfortunately, the cycle length for any star is correlated with the cutoff size used to define the significant outbursts. Using only the largest outbursts and slowest cycles yields a longer mean period (§ 2.5; de Groot, van Genderen, & Sterken 1996; van Genderen, Sterken, & de Groot 1997). If η Car is representative, however, the mean period should probably be based on all of the significant outbursts, which is what we have done. In any case, the periods derived by van Genderen et al. (1997) fall within a factor of 2 of ours, which, considering all the uncertainties, is not a very large difference.

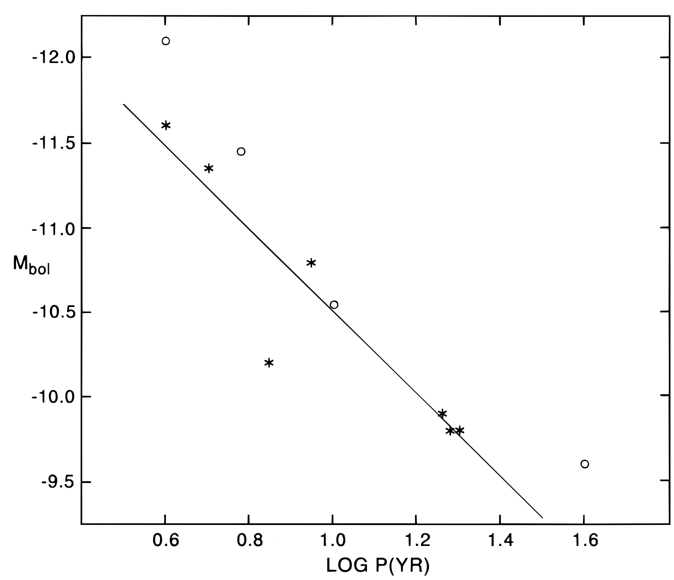

FIG. 4.—Period-luminosity relation for the slow variations observed in seven LBVs (*asterisks*) or predicted from stellar models undergoing recurrent dynamical instability (*open circles*). The straight line represents a fit to the observational points.

We have previously noted that the period-luminosity relation for LBVs may be useful in extragalactic distance studies. Here we expand on this idea by pointing out the serious limitations of two other distance determination methods that likewise have been based on the luminosities of LBVs. The use of LBVs is of greatest service, of course, for remote galaxies that are too distant for the detection of fainter variable stars like Cepheids.

One of the two earlier methods assumes that the absolute magnitudes of the brightest blue stars (which are usually LBVs) in a spiral or irregular galaxy of a given luminosity have an average value that is a universal constant (Hubble 1936; Tammann & Sandage 1968; Sandage & Tammann 1974; de Vaucouleurs 1978; Sandage & Carlson 1985; Humphreys 1987). The problem is that, in practice, only a few bright blue stars constitute a typical observational sample, even for a very rich spiral. The scatter of their absolute magnitudes is potentially very large (Fig. 4), and each star is usually, in addition, irregularly variable. A lesser problem is that, unless the galaxy has a very high luminosity, the average absolute magnitude of the brightest blue stars is correlated with the galaxy's luminosity (a statistical effect). Finally, unless each bright blue star is carefully investigated on an individual basis, it can turn out that contaminating factors such as crowding, duplicity, clustering, presence of field stars, and unrecognized H II regions may be contributing to the measured object's apparent magnitude. Although colorimetric and spectroscopic studies can verify the successful spatial resolution of the brightest blue stars, the fact remains that a group-average absolute magnitude makes a poor basis for a distance determination.

Wolf (1989) pointed out an empirical relation between the absolute bolometric magnitude and the blue-light amplitude of LBVs. Recognizing that the effective temperature of the pseudophotosphere always falls to ~ 8000 K at maximum blue light, Wolf explained his relation by noting that the photospheric effective temperatures of the more luminous LBVs at quiescence are higher than those of fainter LBVs. He thus concluded that the observed blue-light amplitude measures the change of bolometric correction between the dust-free star at minimum blue light and the dust-enshrouded star at maximum blue light. Despite some qualifications expressed about this interpretation (de Koter et al. 1996; de Groot et al. 1996), the relationship itself at least is not in question. It does not apply, however, to luminosities greater than $\sim 1 \times 10^6\ L_\odot$ ($M_{\rm bol} = -10.2$), since the brightest LBVs at quiescence display "apparent" photospheric effective temperatures that do not increase with luminosity. Consequently, Wolf's relation can be used to obtain unambiguous results only in the case of LBVs with not-too-large blue-light amplitudes. This limitation restricts the usefulness of his method to the relatively nearer spiral and irregular galaxies.

8. CONCLUSION

Only a few observational facts are certain about the central object in η Car. If the hot central object is single, its luminosity must be $\sim 5 \times 10^6\ L_\odot$, although, if double, the brighter component might be as faint as $\sim 2.5 \times 10^6\ L_\odot$. The present rate of mass loss from η Car, which hovers in a state somewhere between eruption and quiescence, is (1–3) $\times 10^{-3}\ M_\odot\ {\rm yr}^{-1}$. Major outbursts seem to occur at varying intervals, but roughly once every 3–6 yr. Distant ejecta show measurable overabundances of helium and nitrogen. Except for these few clues, η Car still remains enveloped in a mystery as thick as its nebula.

We have provisionally interpreted η Car as a single (or possibly binary) very massive star, burning hydrogen in its core and repeatedly encountering ionization-induced dynamical instability within its outer envelope. Its original mass must have been 150–300 $M_\odot$, and its prior rate of stellar wind mass loss could not have been too large ($w < 1$). According to our best models, its present mass would be smaller by about one-third. Probably its present surface hydrogen abundance is roughly half of its original value. Although the effective temperature of a star with such a high rate of mass loss is not well defined, the photosphere as conventionally derived using hydrostatic models occurs at $T_e = 8000 \pm 2000$ K for most of our dynamically unstable models. This can be only a lower limit; an extreme upper limit is $T_e \approx 200{,}000$ K (§ 4.1). Possible relaxation oscillations occurring during the most unstable phase and having a period of ~ 0.5 yr would probably be hidden beneath the opaque expanding cloud.

Outbursts in the models succeed each other at unequal intervals, but a typical cycle lasts ~ 4 yr. The computed intervals reflect solely the secular adjustment timescale of the envelope, because they have been derived from a quasi-static evolution code. Even though the mass-ejection timescale and the dynamical timescale approach in length the secular timescale in such highly luminous stars, we believe that our present results are sufficiently realistic to test the ionization-induced dynamical instability mechanism for η Car. Together with our results derived for smaller initial stellar masses, we have been able to confirm our earlier suspicion that the mean cycle time is, approximately, inversely proportional to luminosity, in agreement with observations of LBVs of all luminosities. Nearly all LBVs with $\log (L/L_\odot) < 6.3$, however, are expected to have reached the core helium-burning phase, whereas the brighter ones are probably burning core hydrogen. This accords with the strong environmental evidence for relatively old age among the fainter LBVs as compared to η Car (Gallagher, Kenyon, & Hege 1981; Lortet & Testor 1988).

While the evidence in favor of the ionization-induced dynamical instability mechanism is reasonably strong for ordinary LBVs (Stothers & Chin 1996), this mechanism may nevertheless not be operating in stars with $\log (L/L_\odot) > 6.3$. Chief among possible objections are the very large observed mass-loss rates ($w \approx 3$) for main-sequence stars with masses of $\sim 100\ M_\odot$ (and presumably higher masses), which prevents these stars from ever reaching a state of dynamical instability. The empirical rates of mass loss (de Koter et al. 1997), however, need to be verified. Another possible objection is that our models spend a considerable fraction of their hydrogen-burning lifetimes rather far to the right of the ZAMS in the H-R diagram, until the stage when dynamical instability first sets in. Such cool, very massive stars have not yet been detected observationally. Maybe even our models for η Car itself are too cool. Finally, the observed cycle times of 3–6 yr are not necessarily very discriminating diagnostics of competing theories for stars this massive (§ 7), although they may be. If Damineli (1996) is correct and η Car is a wide, eccentric, interacting binary system with an orbital period of 5.52 yr that accounts for the periodic variability, our mechanism might at most help provide the overall state of destabilization. More likely, our present calculations serve to impose an approximate upper limit on the luminosities at which the ionization-induced dynamical instability mechanism could actually apply. AG Car may be just at this threshold luminosity; an empirical determination of its present mass is badly needed (Stothers & Chin 1995).

An alternative mechanism for producing cycles of mass loss has been examined. It assumes enhanced mass loss due to the supercritical radiative acceleration of matter outward from the photosphere. No repetition of cycles, however, appears in our most luminous stellar models based on this mechanism. However, the potential for supercritical radiative acceleration exists in the appropriate ranges of luminosity and effective temperatures that would apply to η Car and to very hot, luminous objects like it. Moreover, our models are only quasi-static. Since such high rates of quiescent stellar wind mass loss as are observed in η Car might arise from this mechanism and, in any case, must disturb the whole outer envelope, a self-consistent hydrodynamical treatment of both the atmosphere and the outer envelope might reveal slow secular oscillations, whose expected mean cycle time would be ~ 4 yr. The lifetime of this phase cannot much exceed 10^5 yr for such high mass losses, and therefore would be only a small fraction of the star's total hydrogen-burning lifetime of 2×10^6 yr.

Independent of the pros and cons of the two theories discussed above, there remains the problem of the rare episodes of exceptional mass loss, like the 1843 outburst of η Car, which have not yet been plausibly explained by any mechanism.

We thank A. M. van Genderen, an anonymous referee, and our scientific editor, S. N. Shore, for useful suggestions. This work was supported by the NASA Astrophysics Research Program.

APPENDIX

To consider the effect of nonadiabaticity on the stability of a stellar envelope, we adopt Baker's (1966) linearized nonadiabatic one-zone model. Small perturbations of the radius and of other physical quantities are assumed to obey an exponential time dependence, e.g., $\delta r/r_0 \propto \exp(st)$. Our basis for discussion is the dispersion relation given by Baker's cubic equation (29):

$$s^3 + K\sigma_0 As^2 + \sigma_0^2 Bs + K\sigma_0^3 D = 0 . \tag{A1}$$

Here $\sigma_0^2 = GM(r)/r_0^3$; $B = 3\Gamma_1 - 4$; $K = (2\rho L)/(P\delta\sigma_0 \Delta M)$; A, D are functions of the density partial derivatives, $\alpha = (\partial \ln \rho/\partial \ln P)_T$ and $\delta = -(\partial \ln \rho/\partial \ln T)_P$, and of the opacity partial derivatives, $\kappa_T = (\partial \ln \kappa/\partial \ln T)_P$ and $\kappa_P = (\partial \ln \kappa/\partial \ln P)_T$; P is pressure; T is temperature; and ΔM is the mass contained in the single zone. Note that K is a parameter indicating the degree of nonadiabaticity; it is approximately equal to the ratio of the free-fall collapse time (σ_0^{-1}) to the thermal timescale ($E_{\rm th}/L$).

In the adiabatic case ($K = 0$), Baker showed that

$$s = \pm iB^{1/2}\sigma_0 . \tag{A2}$$

If $B > 0$, the solution implies an adiabatic oscillation with period $\Pi_a = 2\pi B^{-1/2}\sigma_0^{-1}$. If $B < 0$, an exponential growth results, with an e-folding time of $\tau_a = |B|^{-1/2}\sigma_0^{-1}$; this implies dynamical instability. The threshold occurs at $\Gamma_1 = 4/3$ ($B = 0$).

In the case of highly nonadiabatic oscillations, Buchler & Regev (1982) pointed out that equation (A1) has the limiting solution

$$s = \pm i(D/A)^{1/2}\sigma_0 . \tag{A3}$$

If $D/A > 0$, a purely nonadiabatic oscillation with a period $\Pi_n = 2\pi(D/A)^{-1/2}\sigma_0^{-1}$ results. If $D/A < 0$, exponential growth occurs with an e-folding time $\tau_n = |D/A|^{-1/2}\sigma_0^{-1}$; this can be interpreted as a dynamical secular instability. Note that the solution depends on the partial derivatives of opacity and density rather than on the adiabatic exponent Γ_1. The purely nonadiabatic oscillation period is, nevertheless, of the same order of magnitude as the purely adiabatic period when $B > 0$, and in both cases the condition for vibrational stability is $AB - D > 0$. Such a purely nonadiabatic mode represents the limiting case of the so-called strange pulsational modes discovered in highly nonadiabatic stellar envelope models (e.g., Wood 1976; Cox et al. 1980; Saio, Wheeler, & Cox 1984; Gautschy & Glatzel 1990; Glatzel 1994).

It is worth emphasizing that, to all orders in the nonadiabaticity (below infinite K), the solution of equation (A1) changes from one of dynamical stability to one of dynamical instability at $B = 0$ (Jeans 1929; Baker 1966). The mathematical proof of this statement is provided by Jeans (1929, § 108), If K is infinite, B becomes irrelevant, and dynamical stability is then determined only by the sign of D/A (Buchler & Regev 1982).

If ordinary dynamical stability prevails ($B > 0$) and the envelope is vibrationally stable, the solution of equation (A1) (omitting the dynamical terms s^3 and s^2) is

$$s = -(D/B)K\sigma_0 . \tag{A4}$$

This solution refers to the familiar criterion for thermal secular instability, $D < 0$; the related e-folding time is of the order of $(K\sigma_0)^{-1}$, the thermal timescale (Baker 1966). As K increases, we find that thermal secular instability goes gradually over into dynamical secular instability.

In massive stars that have a large luminosity-to-mass (L/M) ratio, radiation pressure dominates gas pressure. Denoting by β the fraction of the total pressure contributed by the gas, we find the following proportionalities for small β: $K\sigma_0 \propto \beta^2 L/\Delta M$,

$B \propto \beta$, $A \propto \beta^{-1}$, and $D \propto \beta^{-1}$. It follows from simple inspection of equation (A1) that a massive stellar envelope in which $L/\Delta M$ is large must behave very nonadiabatically. This suggests that when dynamical stability is lost, nonadiabatic behavior will be superimposed on the quasi-adiabatic expansion of the envelope. The opacity partial derivatives actually determine the type of nonadiabatic behavior. Owing to low gas densities, the electron-scattering opacity, which has a simple constant value, dominates the other sources of opacity, and so κ_T and κ_P are small. Under these conditions, $D/A \approx \kappa_T + 4\kappa_P$. Although κ_P is always positive, κ_T may be positive or negative; but the sum $\kappa_T + 4\kappa_P$, is usually positive. In this case, nonadiabatic pulsations occur. Nonlinear hydrodynamical models for LBVs (Stothers & Chin 1993), as well as the earlier models of Tuchman et al. (1978) for dynamically unstable low-mass red giants with very high luminosities, confirm these expectations.

REFERENCES

Allen, D. A. 1979, MNRAS, 189, 1P
Allen, D. A., & Hillier, D. J. 1993, Proc. Astron. Soc. Australia, 10, 338
Allen, D. A., Jones, T. J., & Hyland, A. R. 1985, ApJ, 291, 280
Aller, L. H. 1954, Astrophysics: Nuclear Transformations, Stellar Interiors, and Nebulae (New York: Ronald)
Andriesse, C. D. 1979, Ap&SS, 61, 205
Andriesse, C. D., Donn, B. D., & Viotti, R. 1978, MNRAS, 185, 771
Andriesse, C. D., Packet, W., & de Loore, C. 1981, A&A, 95, 202
Appenzeller, I. 1986, in IAU Symp. 116, Luminous Stars and Associations in Galaxies, ed. C. W. H. de Loore, A. J. Willis, & P. Laskarides (Dordrecht: Reidel), 139
———. 1989, in Physics of Luminous Blue Variables, ed. K. Davidson, A. F. J. Moffat, & H. J. G. L. M. Lamers (Dordrecht: Kluwer), 195
Baker, N. 1966, in Stellar Evolution, ed. R. F. Stein & A. G. W. Cameron (New York: Plenum), 333
Barbá, R. H., Niemela, V. S., Baume, G., & Vazquez, R. A. 1995, ApJ, 446, L23
Bath, G. T. 1979, Nature, 282, 274
Becker, W. 1960, Z. Astrophys., 51, 49
Bisnovatyi-Kogan, G. S. 1973, Ap&SS, 22, 307
Bisnovatyi-Kogan, G. S., & Nadyoshin, D. K. 1972, Ap&SS, 15, 353
Blomme, R., Vanbeveren, D., & Van Rensbergen, W. 1991, A&A, 241, 479
Borgwald, J. M., & Friedlander, M. W. 1993, ApJ, 408, 230
Buchler, J. R., & Regev, O. 1982, A&A, 114, 188
Burbidge, G. R. 1962, ApJ, 136, 304
Burbidge, G. R., & Stein, W. A. 1970, ApJ, 160, 573
Burgarella, D., & Paresce, F. 1991, A&A, 241, 595
Castor, J. I., Abbott, D. C., & Klein, R. I. 1975, ApJ, 195, 157
Conti, P. S. 1984, in IAU Symp. 105, Observational Tests of Stellar Evolution Theory, ed. A. Maeder & A. Renzini (Dordrecht: Reidel), 233
Corcoran, M. F., Rawley, G. L., Swank, J. H., & Petre, R. 1995, ApJ, 445, L121
Cox, J. P., King, D. S., Cox, A. N., Wheeler, J. C., Hansen, C. J., & Hodson, S. W. 1980, Space Sci. Rev., 27, 529
Cox, P., et al. 1995, A&A, 297, 168
Currie, D. G., et al. 1996, AJ, 112, 1115
Damineli, A. 1996, ApJ, 460, L49
Davidson, K. 1971, MNRAS, 154, 415
———. 1987, ApJ, 317, 760
———. 1989, in Physics of Luminous Blue Variables, ed. K. Davidson, A. F. J. Moffatt, & H. J. G. L. M. Lamers (Dordrecht: Kluwer), 101
Davidson, K., Dufour, R. J., Walborn, N. R., & Gull, T. R. 1986, ApJ, 305, 867
Davidson, K., Walborn, N. R., & Gull, T. R. 1982, ApJ, 254, L47
Davidson, K., et al. 1995, AJ, 109, 1784
de Groot, M., van Genderen, A. M., & Sterken, C. 1996, Irish Astron. J., 23, 187
de Jager, C. 1980, The Brightest Stars (Dordrecht: Reidel)
———. 1984, A&A, 138, 246
de Koter, A., Heap, S. R., & Hubeny, I. 1997, ApJ, 477, 792
de Koter, A., Lamers, H. J. G. L. M., & Schmutz, W. 1996, A&A, 306, 501
de Vaucouleurs, G. 1978, ApJ, 224, 14
de Vaucouleurs, G., & Eggen, O. J. 1952, PASP, 64, 185
Doom, C., De Greve, J. P., & de Loore, C. 1986, ApJ, 303, 136
Faulkner, D. J. 1963, PASP, 75, 269
Feast, M. W., Whitelock, P. A., & Warner, B. 1994, A&A, 285, 199
Feinstein, A. 1963, PASP, 75, 492
———. 1969, MNRAS, 143, 273
Feinstein, A., & Marraco, H. G. 1974, A&A, 30, 271
Feinstein, A., Marraco, H. G., & Muzzio, J. C. 1973, A&AS, 12, 331
Forbes, J. E. 1968, ApJ, 153, 495
Forte, J. C. 1978, AJ, 83, 1199
Forte, J. C., & Orsatti, A. M. 1981, AJ, 86, 209
Fusi-Pecci, F., & Renzini, A. 1975, Mém. Soc. R. Sci. Liège (Sér. 6), 6, 383
Gallagher, J. S. 1989, in Physics of Luminous Blue Variables, ed. K. Davidson, A. F. J. Moffatt, & H. J. G. L. M. Lamers (Dordrecht: Kluwer), 185
Gallagher, J. S., Kenyon, S. J., & Hege, E. K. 1981, ApJ, 249, 83
Gautschy, A., & Glatzel, W. 1990, MNRAS, 245, 597
Gaviola, E. 1950, ApJ, 111, 408
Gehrz, R. D., & Ney, E. P. 1972, Sky & Tel., 44, 4
Gehrz, R. D., Ney, E. P., Becklin, E. E., & Neugeubauer, G. 1973, Astrophys. Lett., 13, 89
Glatzel, W. 1994, MNRAS, 271, 66
Glatzel, W., & Kiriakidis, M. 1993a, MNRAS, 262, 85
———. 1993b, MNRAS, 263, 375
Glatzel, W., Kiriakidis, M., & Fricke, K. J. 1994, in Pulsation, Rotation and Mass Loss in Early-Type Stars, ed. L. A. Balona, H. F. Henrichs, & J. M. Le Contel (Dordrecht: Kluwer), 73
Gratton, L. 1963, Star Evolution (New York: Academic), 297
Hamann, F., DePoy, D. L., Johansson, S., & Elias, J. 1994, ApJ, 422, 626
Hansen, C. J. 1978, ARA&A, 16, 15
Herbst, W. 1976, ApJ, 208, 923
Hillier, D. J., & Allen, D. A. 1992, A&A, 262, 153
Hoffleit, D. 1933, Harv. Obs. Bull., No. 893, 11
———. 1956, ApJ, 124, 61
Hoyle, F., Solomon, P. M., & Woolf, N. J. 1973, ApJ, 185, L89
Hubble, E. 1936, The Realm of the Nebulae (New Haven: Yale Univ. Press)
Humphreys, R. M. 1978, ApJS, 38, 309
———. 1987, PASP, 99, 5
Humphreys, R. M., & Davidson, K. 1979, ApJ, 232, 409
———. 1994, PASP, 106, 1025
Hyland, A. R., Robinson, G., Mitchell, R. M., Thomas, J. A., & Becklin, E. E. 1979, ApJ, 233, 145
Iglesias, C. A., Rogers, F. J., & Wilson, B. G. 1992, ApJ, 397, 717
Innes, R. T. A. 1903, Cape Ann., 9, 75B
Jeans, J. H. 1929, Astronomy and Cosmogony (Cambridge: Cambridge Univ. Press)
Kaltcheva, N. T., & Georgiev, L. N. 1993, MNRAS, 261, 847
Kiriakidis, M., Fricke, K. J., & Glatzel, W. 1993, MNRAS, 264, 50
Koenigsberger, G., Guinan, E., Auer, L., & Georgiev, L. 1995, ApJ, 452, L107
Lamers, H. J. G. L. M. 1986, in IAU Symp. 116, Luminous Stars and Associations in Galaxies, ed. C. W. H. de Loore, A. J. Willis, & P. Laskarides (Dordrecht: Reidel), 157
———. 1987, in Instabilities in Luminous Early Type Stars, ed. H. J. G. L. M. Lamers & C. W. H. de Loore (Dordrecht: Reidel), 99
Lamers, H. J. G. L. M., & Fitzpatrick, E. L. 1988, ApJ, 324, 279
Lamers, H. J. G. L. M., et al. 1996, A&A, 315, L225
Langer, N., Hamann, W.-R., Lennon, M., Najarro, F., Pauldrach, A. W. A., & Puls, J. 1994, A&A, 290, 819
Lasker, B. M., & Hesser, J. E. 1972, Nature Phys. Sci., 237, 73
Ledoux, P. 1958, in Handbuch der Physik, Vol. 51, ed. S. Flügge (Berlin: Springer), 605
Leitherer, C., Schmutz, W., Abbott, D. C., Hamann, W. R., & Wessolowski, U. 1989, ApJ, 346, 919
Leitherer, C., et al. 1994, ApJ, 428, 292
Levato, H., & Malaroda, S. 1982, PASP, 94, 807
Levenson, N. A., Kirshner, R. P., Blair, W. P., & Winkler, P. F. 1995, AJ, 110, 739
Lobel, A., Achmad, L., de Jager, C., & Nieuwenhuijzen, H. 1992, A&A, 264, 147
Lortet, M.-C., & Testor, G. 1988, A&A, 194, 11
Lucy, L. B., & Abbott, D. C. 1993, ApJ, 405, 738
Maeder, A. 1980, A&A, 92, 101
———. 1983, A&A, 120, 113
———. 1989, in Physics of Luminous Blue Variables, ed. K. Davidson, A. F. J. Moffatt, & H. J. G. L. M. Lamers (Dordrecht: Kluwer), 15
——— 1992, in Instabilities in Evolved Super- and Hypergiants, ed. C. de Jager & H. Nieuwenhuijzen (Amsterdam: North-Holland), 138
Massey, P., & Johnson, J. 1993, AJ, 105, 980
Meaburn, J., Walsh, J. R., & Wolstencroft, R. D. 1993, A&A, 268, 283
Men'schikov, A. B., Tutukov, A. V., & Shustov, B. M. 1989, Soviet Astron., 33, 416
Nieuwenhuijzen, H., & de Jager, C. 1990, A&A, 231, 134
O'Connell, D. J. K. 1956, Vistas Astron., 2, 1165
Ostriker, J. P., & Gunn, J. E. 1971, ApJ, 164, L95
Pagel, B. E. J. 1969, Astrophys. Lett., 4, 221
Payne-Gaposchkin, C. 1957, The Galactic Novae (Amsterdam: North-Holland)
Polcaro, V. F., & Viotti, R. 1993, A&A, 274, 807
Pottasch, S. R., Wesselius, P. R., & van Duinen, R. J. 1976, A&A, 47, 443
Robberto, M., Ferrari, A., Nota, A., & Paresce, F. 1993, A&A, 269, 330
Rodgers, A. W., & Searle, L. 1967, MNRAS, 135, 99
Saio, H., Wheeler, J. C., & Cox, J. P. 1984, ApJ, 281, 318
Sandage, A., & Carlson, G. 1985, AJ, 90, 1464
Sandage, A., & Tammann, G. A. 1974, ApJ, 191, 603

Shobbrook, R. R., & Lyngå, G. 1994, MNRAS, 269, 857
Simon, N. R., & Stothers, R. B. 1970, A&A, 6, 183
Smith, C. H., Aitken, D. K., Moore, T. J. T., Roche, P. F., Puetter, R. C., & Piña, R. K. 1995, MNRAS, 273, 354
Sterken, C., de Groot, M. J. H., & van Genderen, A. M. 1996, A&AS, 116, 9
Stothers, R. B. 1992, ApJ, 392, 706
Stothers, R. B., & Chin, C.-w. 1979, ApJ, 233, 267
———. 1983, ApJ, 264, 583
———. 1993, ApJ, 408, L85
———. 1994, ApJ, 426, L43
———. 1995, ApJ, 451, L61
———. 1996, ApJ, 468, 842
Talbot, R. 1971, ApJ, 165, 121
Tammann, G. A., & Sandage, A. 1968, ApJ, 151, 825
Tapia, M., Roth, M., Marraco, H., & Ruiz, M. T. 1988, MNRAS, 232, 661
Thackeray, A. D. 1953, MNRAS, 113, 211
———. 1956, Observatory, 76, 103
———. 1961, Observatory, 81, 99
———. 1974, MNRAS, 168, 221
Thé, P. S., Bakker, R., & Antalova, A. 1980, A&AS, 41, 93
Thé, P. S., & Vleeming, G. 1971, A&A, 14, 120
Tovmasyan, G. M., Oganesyan, R. K., & Epremyan, R. A. 1993, Soviet Astron. Lett., 18, 369
Tuchman, Y., Sack, N., & Barkat, Z. 1978, ApJ, 219, 183
Turner, D. G., & Moffat, A. F. J. 1980, MNRAS, 192, 283
Tutukov, A. V., & Yungel'son, L. R. 1980, Soviet Astron. Lett., 6, 271
van Genderen, A. M., de Groot, M. J. H., & Thé, P. S. 1994, A&A, 283, 89
van Genderen, A. M., Sterken, C., & de Groot, M. 1997, A&A, 318, 81
van Genderen, A. M., & Thé, P. S. 1984, Space Sci. Rev., 39, 317
van Genderen, A. M., et al. 1995, A&A, 304, 415
Viotti, R., & Andresse, C. D. 1981, in The Most Massive Stars, ed. S. D'Odorico, D. Baade, & K. Kjar (Garching: ESO), 141
Viotti, R., Rossi, L., Cassatella, A., Altamore, A., & Baratta, G. B. 1989, ApJS, 71, 983
Walborn, N. R. 1973, ApJ, 179, 517
Walborn, N. R., Blanco, B. M., & Thackeray, A. D. 1978, ApJ, 219, 498
Walborn, N. R., & Hesser, J. E. 1975, ApJ, 199, 535
Walborn, N. R., & Liller, M. 1977, ApJ, 211, 181
Warren-Smith, R. F., Scarrott, S. M., Murdin, P., & Bingham, R. G. 1979, MNRAS, 187, 761
White, S. M., Duncan, R. A., Lim, J., Nelson, G. J., Drake, S. A., & Kundu, M. R. 1994, ApJ, 429, 380
Whitelock, P. A., Feast, M. W., Koen, C., Roberts, G., & Carter, B. S. 1994, MNRAS, 270, 364
Wolf, B. 1989, A&A, 217, 87
Wolf, B., & Stahl, O. 1982, A&A, 112, 111
Wood, P. R. 1976, MNRAS, 174, 531
Zwicky, F. 1965, in Stellar Structure, ed. L. H. Aller & D. B. McLaughlin (Chicago: Univ. Chicago Press), 367